



# Measurements of coeluting unlabeled and $^{13}\text{C}$ -labeled polychlorinated biphenyl congeners with partially overlapping fragment profiles using a tandem mass spectrometry

Ji-Zhong Wang<sup>a</sup>, Ze-Yu Yang<sup>b</sup>, Eddy Y. Zeng<sup>a,\*</sup>

<sup>a</sup> State Key Laboratory of Organic Geochemistry, Guangzhou Institute of Geochemistry, Chinese Academy of Sciences, Guangzhou 510640, China

<sup>b</sup> School of Environmental Studies, China University of Geosciences, Wuhan 430074, China

## ARTICLE INFO

### Article history:

Received 7 November 2009

Received in revised form 16 January 2010

Accepted 18 January 2010

Available online 25 January 2010

### Keywords:

Tandem mass spectrometry

Quantitation error

Coexisting ion

Polychlorinated biphenyls

## ABSTRACT

$^{13}\text{C}$ -labeled compounds are often employed as surrogate or internal standards to monitor the performance of extraction and instrumental analysis procedures for their unlabeled counterparts. However, labeled and unlabeled counterparts most often coelute chromatographically with overlapping mass ion fragments, posing a challenge to the accurate quantification of these compounds. In the present study, an analytical scheme, using coeluting unlabeled and  $^{13}\text{C}$ -labeled polychlorinated biphenyl (PCB) congeners as the model compounds, was developed with a low-resolution tandem mass spectrometer (MS/MS) to determine the appropriate ranges of PCB congener concentrations that satisfy the no-interference condition. Interferences from unlabeled PCBs to quantitation of labeled counterparts could be minimized when  $^{13}\text{C}$ -labeled PCB congeners were quantified in the MS/MS mode within a certain concentration range. In addition, good agreements between the measured and theoretically predicted quantitation errors were observed for all labeled PCB congeners except PCB 180. The exception with labeled PCB 180 was mainly attributed to the occurrence of instrumental analytical uncertainty, as analytical error was also observed with absence of unlabeled PCB 180. These results indicate that MS/MS techniques can serve as a useful tool to minimize interferences with quantitation of isotopically labeled compounds from their unlabeled counterparts, which possess partially overlapping ion fragment profiles.

© 2010 Elsevier B.V. All rights reserved.

## 1. Introduction

In a conventional analytical method for trace organic compounds, internal and surrogate standards are often used to mitigate analytical uncertainties [1–3]. Stable isotope labeled compounds, such as deuterated or  $^{13}\text{C}$ -labeled counterparts of the target analytes, are often regarded as the best candidates of internal or surrogate standards due to their similar physicochemical properties to the target analytes. However, as described in previous studies [4–6], deuterated or  $^{13}\text{C}$ -labeled non-halogenated hydrocarbons can be mass spectrally differentiated from their unlabeled counterparts due to the low natural isotopic abundances of the compositional elements (C and H). It is obviously the case for halogenated compounds, e.g., polychlorinated biphenyls (PCBs) or polybrominated diphenyl ethers (PBDEs). The unlabeled and labeled congener pairs coelute chromatographically [7,8], and some pairs may share similar ion fragment profiles resulting from the abundant halogen isotopes [9,10]. This problem can be solved

by employing selective instruments such as high-resolution mass spectrometry (HRMS) [11], multidimensional gas chromatography (GC) [12], or hyphenated instruments with some multivariate data resolution techniques [13,14] and chemometric algorithms [9,15,16]. However, they cannot be widely adopted because of high cost and complicated operational procedures.

Recently, a numerical scheme based upon a two-component model was developed by our group [9], which suggests that theoretical predications can be utilized to determine the appropriate concentration ranges of the coeluting compounds that satisfy the no-interference condition, and the quantitation errors resulting from the partially overlapping mass profiles can be negligible within the appropriate range of concentrations even if only low-resolution mass spectrometers are available. However, the complex model derivation requires qualified personnel, and the variable sample matrix interferences and versatile levels of target analytes make it difficult to select the proper spiking concentrations of surrogate and internal standards.

Several researchers have introduced GC coupled with ion trap mass spectrometry (MS) as an interesting alternative for separating coeluting PCB isomers based on its GC/MS/MS functionality [15,17,18], which has the benefits of high selectivity and stability

\* Corresponding author. Tel.: +86 20 85291421; fax: +86 20 85290706.  
E-mail address: [eddyzeng@gig.ac.cn](mailto:eddyzeng@gig.ac.cn) (E.Y. Zeng).

to facilitate structural recognition for unknown organic chemicals [19]. However, the scope of quantitation errors resulting from different concentration ranges of coeluting isotopically labeled and unlabeled compounds in the GC/MS/MS system has not been dealt with in detail.

To assess the utility of a low-resolution MS/MS system in minimizing quantitation errors for the labeled and unlabeled counterparts of PCB congeners with overlapping mass profiles, five unlabeled PCB congeners (153, 180, 202, 206 and 209) and their  $^{13}\text{C}$ -labeled counterparts (Table 1) were prepared in four sets of standard solutions and analyzed. The MS/MS operational parameters, e.g., the type of precursors and product ions used for ionization and quantitation, and excitation voltage, were optimized to achieve the best possible instrumental sensitivity and selectivity. The mechanisms for elimination of the mutual interferences with quantitation of a given pair of labeled and unlabeled counterparts were examined based upon the probability and combination theory.

## 2. Experimental

### 2.1. Materials

Organic solvents, i.e., hexane, toluene and dichloromethane (DCM) of pesticide grade, were purchased from Sigma–Aldrich (Seelze, Germany) and used as supplied. Individual unlabeled PCB congener standards in solid form were obtained from AccuStandard (New Haven, CT, USA).  $^{13}\text{C}$ -labeled PCB congeners at 40  $\mu\text{g}/\text{mL}$  in nonane were purchased from Cambridge Isotope Laboratories (Andover, MA, USA). Prior to use, all glasswares were cleaned using a multi-step protocol, including hand-washing with detergent and tap water, rinsing with deionized water and kiln-firing at 450  $^{\circ}\text{C}$  for at least 4 h.

### 2.2. Preparation of standard solutions and analytical scheme

Unlabeled PCB congeners were dissolved in toluene, followed by dilution to 50  $\mu\text{g}/\text{mL}$  with hexane.  $^{13}\text{C}$ -labeled PCB congeners were diluted to 2  $\mu\text{g}/\text{mL}$  with hexane. These stock solutions, stored at  $-20^{\circ}\text{C}$ , were used to prepare working solutions with hexane before instrumental analysis. Overall, four sets of working solutions were prepared. The first set (series A) contained the unlabeled PCB congeners at 40 ng/mL and the  $^{13}\text{C}$ -labeled PCB counterparts at 10, 20, 30, 40 and 50 ng/mL, respectively (i.e., five solutions). The second set (series B) contained the  $^{13}\text{C}$ -labeled PCB congeners at 10, 20, 30, 40 and 50 ng/mL, respectively, and their unlabeled PCB counterparts at 1000 ng/mL. Series A and B were analyzed with both the selected ion storage (SIS) mode and MS/MS mode with the unlabeled PCB counterparts as the internal standards. The objectives were to identify the magnitude of interferences resulting from the unlabeled PCB counterparts for the calibration of each  $^{13}\text{C}$ -labeled PCB congener by examining the linear regression correlation coefficients ( $R^2$ ) and relative standard deviations (RSDs). The third set (series C) contained  $^{13}\text{C}$ -labeled PCB analytes at 10, 50, 100, 200 and 500 ng/mL, respectively, with unlabeled PCB 197 at 200 ng/mL. PCB 197 was used as the internal standard to monitor the instrumental performance, because it could be separated chromatographically from all  $^{13}\text{C}$ -labeled PCB analytes. The fourth set (series D) contained the  $^{13}\text{C}$ -labeled PCB congeners at a fixed concentration of 20 ng/mL and the unlabeled PCB counterparts at 0, 500, 1000, 2000, 4000 and 10,000 ng/mL, respectively, as well as unlabeled PCB 197 at 200 ng/mL in all standard solutions. Series C and D were analyzed with the MS/MS method only, and unlabeled PCB 197 was analyzed in the SIS mode for all solutions. The linear calibration graphs for series C were established to quantify the results from the analyses of series D. Standard solutions in series D

were analyzed with the MS/MS procedure in seven repeated runs. The measured concentration and experimentally measured quantitation error ( $E'$ (%)) for each  $^{13}\text{C}$ -labeled PCB model compound were calculated to ascertain the magnitude of interferences from their unlabeled PCB counterparts at different levels. On the other hand,  $E'$ (%) was calculated by the measured concentration and the known spiked concentration:

$$E'(\%) = \frac{|C_2' - C_2^{\text{spiked}}|}{C_2^{\text{spiked}}} \times 100 \quad (1)$$

where  $C_2'$  and  $C_2^{\text{spiked}}$  are the measured and the known spiked (20 ng/mL) concentration of a  $^{13}\text{C}$ -labeled PCB model compound, respectively.

### 2.3. GC/MS analysis

The instrumental analysis scheme was described elsewhere [9,20]. Briefly, a Varian 3800 gas chromatograph/Saturn 2000 ion trap mass spectrometer was employed for peak identification and quantitation, and a 60 m  $\times$  0.25 mm-i.d. (0.25  $\mu\text{m}$  film thickness) DB-5MS column (J&W Scientific, Folsom, CA, USA) was used for separation. Column temperature was programmed from 100  $^{\circ}\text{C}$  with a hold of 1 min, increased to 220  $^{\circ}\text{C}$  at 8  $^{\circ}\text{C}/\text{min}$  and ramped at 10  $^{\circ}\text{C}/\text{min}$  to the final temperature of 290  $^{\circ}\text{C}$  (held for 10 min). Helium was employed as the carrier gas, with a constant flow of 1.3 mL/min. Extract injection was conducted in the splitless/split mode with a split time of 3 min. The injection port, ion trap, manifold and transfer line temperatures were maintained at 280, 190, 40 and 280  $^{\circ}\text{C}$ , respectively. Mass fragments were generated in the positive electron impact mode at an electron voltage of 70 eV and scanned in the total ion scan mode within the range of  $m/z$  100–550. The target analytes were quantified in SIS mode and MS/MS mode, respectively, and the scan range and quantitation ions are presented in Table 1.

Automatic gain control target value, emission current, isolation width, isolation and excitation times and  $q$  value were optimized according to the instrumental specification to achieve favorable resolution, mass accuracy and operation performance. The excitation amplitude was adjusted to obtain an ideal daughter ion by an automated method development (AMD) tool at the resonant mode using a standard solution containing unlabeled PCB congeners at 500 ng/mL, with a gradual increase of collision-induced-dissociation (CID) voltage up to 10 scans per cycle. Different excitation voltages from 0.5 to 3.0 eV were tried in the AMD mode to minimize the intensities of precursors while maximizing those of daughter ions (Fig. 1). The most abundant ions were selected as the final daughter ions for each target analyte in the MS/MS mode (Table 1). As the excitation voltage was scanned from 0.5 to 3.0 eV, the quantitation ions with highest abundances were used to select the optimal excitation voltages for the target analytes (Fig. 1). As a result, the excitation voltages employed in the present study were 1.2 eV for PCB 153, 1.5 eV for PCB 180, 202 and 209 and 2.2 eV for PCB 206. The same selection was also applicable to  $^{13}\text{C}$ -labeled PCB counterparts.

All of the linear calibration graphs were constructed by least-squares regression of the concentration versus peak area ratios of the calibration standards. In brief, the relative response ( $\text{RR}_X$ ) of each PCB congener was calculated for each injection by:

$$\text{RR}_X = \frac{R_X C_{\text{IS}}}{R_{\text{IS}} C_X} \quad (2)$$

where  $R_X$  and  $R_{\text{IS}}$  represent the responses of compound X and the internal standard, respectively, and  $C_X$  and  $C_{\text{IS}}$  are the concentrations of compound X and the internal standard, respectively.

**Table 1**  
The scan and quantitation (quant.) ion range employed for analysis of five pairs of unlabeled PCB congener and their  $^{13}\text{C}$ -labeled PCB counterparts in both the GC–MS (selected ion storage mode; SIS) and GC–MS/MS modes.

Compound	$R_t$ (min)	SIS mode				MS/MS mode			
		Unlabeled		$^{13}\text{C}$ -labeled		Unlabeled		$^{13}\text{C}$ -labeled	
		Scan range	Quant. ions	Scan range	Quant. ions	Parent ions	Quant. ions	Parent ions	Quant. ions
PCB 153	28.5	358–370	358–362	370–382	370–374	360	278+280	372	298+300
PCB 180	34.2	392–406	392–398	404–418	404–410	394	322+324	406	334+336
PCB 202	33.0	426–442	428–434	438–454	438–444	430	358+360	442	370+372
PCB 206	41.2	460–478	460–466	472–490	472–478	464	392+394	476	404+406
PCB 209	43.2	494–514	496–502	506–526	506–514	498	426+428	510	438+440
PCB 197	34.0	394–404	428–432						

Because the instrument parameters were maintained constant during injections,  $\text{RR}_X$  should be a relatively fixed value for each congener.

### 3. Theoretical analysis

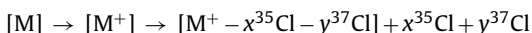
The theoretical relative abundance of a chlorine isotope spectrum can be described by [21]:

$$x_k = \frac{n!}{k!(n-k)!} \times 0.325^k \quad (3)$$

where  $x_k$  is defined as the theoretical relative abundance of an ion fragment with the number of  $^{37}\text{Cl}$  being  $k$  ( $k=0, 1, 3, n$ ), and  $n$  is the total number of chlorines in the ion fragment. In fact, the relative abundance can be expressed by a relative ratio ( $r_k$ ):

$$r_k = \frac{x_k}{\sum x_k} \quad (4)$$

To predict the quantitation error from the coexisting parent ion profile of an given unlabeled PCB congener, a  $^{13}\text{C}$ -labeled PCB parent ion is defined as  $^{13}\text{C}_{12}^{35}\text{Cl}_n^{37}\text{Cl}_m\text{H}_{(10-n-m)}$  or [M]. When [M] is ionized and dissociated,  $x$   $^{35}\text{Cl}$  atoms ( $0 \leq x \leq n$ ) and  $y$   $^{37}\text{Cl}$  atoms ( $0 \leq y \leq m$ ) are lost, producing daughter ions as shown below:



The probability ( $P_2$ ) for losing  $x$   $^{35}\text{Cl}$  and  $y$   $^{37}\text{Cl}$  atoms simultaneously from their parent ions can be calculated as:

$$P_2 = \frac{C_n^x C_m^y}{C_{n+m}^{x+y}} \quad (5)$$

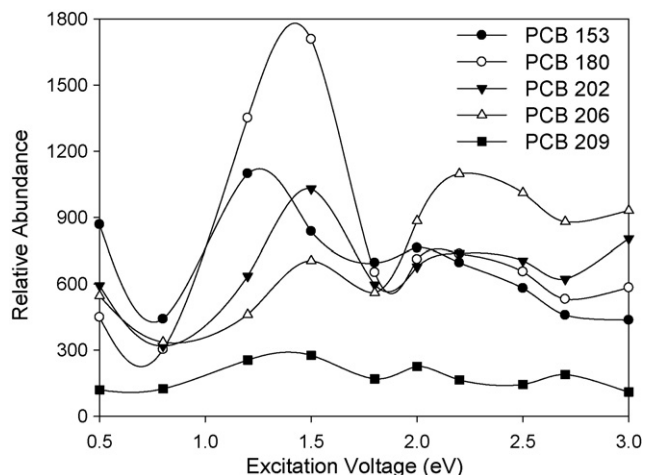


**Fig. 1.** Relative abundances of daughter ions versus resonance excitation voltage (eV) for five  $^{13}\text{C}$ -labeled PCB congeners.

where  $C_n^x$  is the number of  $x$  combinations for losing  $x$  ( $0 \leq x \leq n$ )  $^{35}\text{Cl}$  atoms from a group of  $n$   $^{35}\text{Cl}$  atoms,  $C_m^y$  is the number of  $y$  combinations for losing  $y$   $^{37}\text{Cl}$  atoms from a group of  $m$   $^{37}\text{Cl}$  atoms,  $C_{m+n}^{x+y}$  is the number of  $(x+y)$  Cl atoms, including  $^{35}\text{Cl}$  and  $^{37}\text{Cl}$  atoms and  $0 \leq x+y \leq n+m$ , from a group of  $(m+n)$  Cl atoms ( $^{35}\text{Cl}$  and  $^{37}\text{Cl}$ ).

It is obvious that the same parent ions from the unlabeled counterparts can also dissociate Cl atoms. Correspondingly, the probability ( $P_1$ ) of losing  $s$   $^{35}\text{Cl}$  and  $t$   $^{37}\text{Cl}$  atoms from unlabeled PCB congeners (including  $u$   $^{35}\text{Cl}$  and  $v$   $^{37}\text{Cl}$  atoms) is described by:

$$P_1 = \frac{C_u^s C_v^t}{C_{u+v}^{s+t}} \quad (6)$$

When mass fragment ions overlap, then  $u=m-6$  and  $v=n+6$ . On the other hand, when  $s=x$  and  $t=y$ , the daughter ions from a  $^{13}\text{C}$ -labeled PCB congener and its unlabeled counterpart have the same mass weight, probably resulting in quantitation errors. Therefore, if the most abundant product ions which have coexisting ions from unlabeled PCB congeners are selected as the quantitation ions, the quantitation error (herein, it should be named as the theoretically predicted quantitation error,  $E(\%)$ ) contributed from the coexisting ions of the unlabeled PCB congener when its  $^{13}\text{C}$ -labeled counterpart is quantified can be estimated as:

$$E(\%) = \frac{r_{n+6}(1)P_1C_1}{r_n(2)P_2C_2} \times 100\% = \frac{r_{n+6}(1)P_1}{r_n(2)P_2} C_t \times 100\% \quad (7)$$

where  $E(\%)$  is the relative quantitation error,  $C_1$  and  $C_2$  are the concentrations of the unlabeled and  $^{13}\text{C}$ -labeled PCB congeners, respectively, and  $C_t$  is defined as the ratio of  $C_1/C_2$ . If multiple daughter ions are selected as the quantitation ions, Eq. (7) can be revised to:

$$E(\%) = \frac{r_{n+6}(1) \sum P_1(k)}{r_n(2) \sum P_2(k)} C_t \times 100\% \quad (8)$$

where  $k$  represents the total number of selected quantitation ions. If  $E(\%)$  is set at 15%,  $C_t$  must satisfy the following constraints:

$$C_t < 0.15 \frac{r_n(2)P_2}{r_{n+6}(1)P_1} \quad \text{or} \quad C_t < 0.15 \frac{r_n(2) \sum P_2(k)}{r_{n+6}(1) \sum P_1(k)} \quad (9)$$

## 4. Results and discussion

### 4.1. Theoretical prediction of quantitation errors

If the unlabeled and  $^{13}\text{C}$ -labeled PCB counterparts have the same numbers of  $^{35}\text{Cl}$  and  $^{37}\text{Cl}$  atoms, i.e.,  $r_k(1)=r_k(2)$ , the relative abundance ratios of the selected model compounds can be calculated with Eq. (3) (Table 2). In general, the fragment ions with 1–2  $^{37}\text{Cl}$  atoms have the largest relative abundances. Fragments with high  $r_k$  value are often used as quantitation ions in a conventional MS analysis in the electron impact mode [9] or used as parent ions to generate daughter fragment ions in a tandem MS/MS system [10,22–25]. Accordingly, when the ions from the

**Table 2**

The molecular formula, molecular weight, the ratio of relative abundance between the unlabeled ( $r_1(k)$ ) and  $^{13}\text{C}$ -labeled PCB counterparts ( $r_2(k)$ ), total coexisting ions, parent ions in the MS/MS mode and coexisting ions existing in parent ions.

Compound	Formula	Molecular weight	$r_1/r_2^a$	Total coexisting ions	Parent ion		Coexisting ion						
					UN <sup>b</sup>	L <sup>c</sup>	UN	L					
PCB 153	$^{12}\text{C}_{12}/^{13}\text{C}_{12}^{35}\text{Cl}_6\text{H}_4^d$	358/370 <sup>e</sup>	$1.8 \times 10^{-1}$	370	360	372	No <sup>f</sup>	No					
	$^{12}\text{C}_{12}/^{13}\text{C}_{12}^{35}\text{Cl}_5^{37}\text{ClH}_4$	360/372	$3.6 \times 10^{-1}$										
	$^{12}\text{C}_{12}/^{13}\text{C}_{12}^{35}\text{Cl}_4^{37}\text{Cl}_2\text{H}_4$	362/374	$2.9 \times 10^{-1}$										
	$^{12}\text{C}_{12}/^{13}\text{C}_{12}^{35}\text{Cl}_3^{37}\text{Cl}_3\text{H}_4$	364/376	$1.3 \times 10^{-1}$										
	$^{12}\text{C}_{12}/^{13}\text{C}_{12}^{35}\text{Cl}_2^{37}\text{Cl}_4\text{H}_4$	366/378	$3.0 \times 10^{-2}$										
	$^{12}\text{C}_{12}/^{13}\text{C}_{12}^{35}\text{Cl}^{37}\text{Cl}_5\text{H}_4$	368/380	$4.0 \times 10^{-3}$										
	$^{12}\text{C}_{12}/^{13}\text{C}_{12}^{37}\text{Cl}_6\text{H}_4$	370/382	$2.2 \times 10^{-4}$										
PCB 180	$^{12}\text{C}_{12}/^{13}\text{C}_{12}^{35}\text{Cl}_7\text{H}_3$	392/404	$1.4 \times 10^{-1}$	404	394	406	No	406					
	$^{12}\text{C}_{12}/^{13}\text{C}_{12}^{35}\text{Cl}_6^{37}\text{ClH}_3$	394/406	$3.2 \times 10^{-1}$										
	$^{12}\text{C}_{12}/^{13}\text{C}_{12}^{35}\text{Cl}_5^{37}\text{Cl}_2\text{H}_3$	396/408	$3.1 \times 10^{-1}$	406									
	$^{12}\text{C}_{12}/^{13}\text{C}_{12}^{35}\text{Cl}_4^{37}\text{Cl}_3\text{H}_3$	398/410	$1.7 \times 10^{-1}$										
	$^{12}\text{C}_{12}/^{13}\text{C}_{12}^{35}\text{Cl}_3^{37}\text{Cl}_4\text{H}_3$	400/412	$5.4 \times 10^{-2}$										
	$^{12}\text{C}_{12}/^{13}\text{C}_{12}^{35}\text{Cl}_2^{37}\text{Cl}_5\text{H}_3$	402/414	$1.1 \times 10^{-2}$										
	$^{12}\text{C}_{12}/^{13}\text{C}_{12}^{35}\text{Cl}^{37}\text{Cl}_6\text{H}_3$	404/416	$1.2 \times 10^{-3}$										
	$^{12}\text{C}_{12}/^{13}\text{C}_{12}^{37}\text{Cl}_7\text{H}_3$	406/418	$5.3 \times 10^{-5}$										
	PCB 202	$^{12}\text{C}_{12}/^{13}\text{C}_{12}^{35}\text{Cl}_8\text{H}_2$	426/438	$1.1 \times 10^{-1}$					438	430	442	No	442
$^{12}\text{C}_{12}/^{13}\text{C}_{12}^{35}\text{Cl}_7^{37}\text{ClH}_2$		428/440	$2.7 \times 10^{-1}$										
$^{12}\text{C}_{12}/^{13}\text{C}_{12}^{35}\text{Cl}_6^{37}\text{Cl}_2\text{H}_2$		430/442	$3.1 \times 10^{-1}$	442									
$^{12}\text{C}_{12}/^{13}\text{C}_{12}^{35}\text{Cl}_5^{37}\text{Cl}_3\text{H}_2$		432/444	$2.0 \times 10^{-1}$										
$^{12}\text{C}_{12}/^{13}\text{C}_{12}^{35}\text{Cl}_4^{37}\text{Cl}_4\text{H}_2$		434/446	$8.2 \times 10^{-2}$										
$^{12}\text{C}_{12}/^{13}\text{C}_{12}^{35}\text{Cl}_3^{37}\text{Cl}_5\text{H}_2$		436/448	$2.1 \times 10^{-2}$										
$^{12}\text{C}_{12}/^{13}\text{C}_{12}^{35}\text{Cl}_2^{37}\text{Cl}_6\text{H}_2$		438/450	$3.5 \times 10^{-3}$										
$^{12}\text{C}_{12}/^{13}\text{C}_{12}^{35}\text{Cl}^{37}\text{Cl}_7\text{H}_2$		440/452	$3.2 \times 10^{-4}$										
$^{12}\text{C}_{12}/^{13}\text{C}_{12}^{37}\text{Cl}_8\text{H}_2$		442/454	$1.3 \times 10^{-5}$										
PCB 206		$^{12}\text{C}_{12}/^{13}\text{C}_{12}^{35}\text{Cl}_9\text{H}$	460/472	$7.9 \times 10^{-2}$	472	464	476	No	476				
		$^{12}\text{C}_{12}/^{13}\text{C}_{12}^{35}\text{Cl}_8^{37}\text{ClH}$	462/474	$2.3 \times 10^{-1}$									
	$^{12}\text{C}_{12}/^{13}\text{C}_{12}^{35}\text{Cl}_7^{37}\text{Cl}_2\text{H}$	464/476	$3.0 \times 10^{-1}$	474									
	$^{12}\text{C}_{12}/^{13}\text{C}_{12}^{35}\text{Cl}_6^{37}\text{Cl}_3\text{H}$	466/478	$2.3 \times 10^{-1}$										
	$^{12}\text{C}_{12}/^{13}\text{C}_{12}^{35}\text{Cl}_5^{37}\text{Cl}_4\text{H}$	468/480	$1.1 \times 10^{-1}$										
	$^{12}\text{C}_{12}/^{13}\text{C}_{12}^{35}\text{Cl}_4^{37}\text{Cl}_5\text{H}$	470/482	$3.6 \times 10^{-2}$										
	$^{12}\text{C}_{12}/^{13}\text{C}_{12}^{35}\text{Cl}_3^{37}\text{Cl}_6\text{H}$	472/484	$7.9 \times 10^{-3}$										
	$^{12}\text{C}_{12}/^{13}\text{C}_{12}^{35}\text{Cl}_2^{37}\text{Cl}_7\text{H}$	474/486	$1.1 \times 10^{-3}$										
	$^{12}\text{C}_{12}/^{13}\text{C}_{12}^{35}\text{Cl}^{37}\text{Cl}_8\text{H}$	476/488	$8.9 \times 10^{-5}$										
	$^{12}\text{C}_{12}/^{13}\text{C}_{12}^{37}\text{Cl}_9\text{H}$	478/490	$3.2 \times 10^{-6}$										
	PCB 209	$^{12}\text{C}_{12}/^{13}\text{C}_{12}^{35}\text{Cl}_{10}$	494/506	$6.0 \times 10^{-2}$	506					498	510	No	510
		$^{12}\text{C}_{12}/^{13}\text{C}_{12}^{35}\text{Cl}_9^{37}\text{Cl}$	496/508	$1.9 \times 10^{-1}$									
		$^{12}\text{C}_{12}/^{13}\text{C}_{12}^{35}\text{Cl}_8^{37}\text{Cl}_2$	498/510	$2.8 \times 10^{-1}$	508								
$^{12}\text{C}_{12}/^{13}\text{C}_{12}^{35}\text{Cl}_7^{37}\text{Cl}_3$		500/512	$2.5 \times 10^{-1}$										
$^{12}\text{C}_{12}/^{13}\text{C}_{12}^{35}\text{Cl}_6^{37}\text{Cl}_4$		502/514	$1.4 \times 10^{-1}$										
$^{12}\text{C}_{12}/^{13}\text{C}_{12}^{35}\text{Cl}_5^{37}\text{Cl}_5$		504/516	$5.5 \times 10^{-2}$										
$^{12}\text{C}_{12}/^{13}\text{C}_{12}^{35}\text{Cl}_4^{37}\text{Cl}_6$		506/518	$1.5 \times 10^{-2}$										
$^{12}\text{C}_{12}/^{13}\text{C}_{12}^{35}\text{Cl}_3^{37}\text{Cl}_7$		508/520	$2.8 \times 10^{-3}$										
$^{12}\text{C}_{12}/^{13}\text{C}_{12}^{35}\text{Cl}_2^{37}\text{Cl}_8$		510/522	$3.4 \times 10^{-4}$										
$^{12}\text{C}_{12}/^{13}\text{C}_{12}^{35}\text{Cl}^{37}\text{Cl}_9$		512/525	$2.2 \times 10^{-5}$										
$^{12}\text{C}_{12}/^{13}\text{C}_{12}^{37}\text{Cl}_{10}$		514/526	$7.9 \times 10^{-7}$										

<sup>a</sup>  $r_1$  and  $r_2$  represent the relative abundances of an ion fragment with  $k$  ( $k=0, 1, 3, n$ )  $^{37}\text{Cl}$  atoms for unlabeled and  $^{13}\text{C}$ -labeled PCB counterparts, respectively, calculated by Eq. (3), and  $k$  is the number of  $^{37}\text{Cl}$  atoms. If  $k$  is the same for unlabeled and  $^{13}\text{C}$ -labeled PCB counterparts, then  $r_1(k) = r_2(k)$ .

<sup>b</sup> The coexisting fragment ion from  $^{13}\text{C}$ -labeled PCB congeners with the parent ion of unlabeled PCB counterparts.

<sup>c</sup> The coexisting fragment ion from unlabeled PCB congeners with the parent ion of  $^{13}\text{C}$ -labeled PCB counterparts.

<sup>d</sup>  $^{12}\text{C}_{12}/^{13}\text{C}_{12}^{35}\text{Cl}_6\text{H}_4$  represents the molecular formula of  $^{12}\text{C}_{12}^{35}\text{Cl}_6\text{H}_4$  and  $^{13}\text{C}_{12}^{35}\text{Cl}_6\text{H}_4$ .

<sup>e</sup> 358 is the molecular weight of  $^{12}\text{C}_{12}^{35}\text{Cl}_6\text{H}_4$  and 370 is the molecular weight of  $^{13}\text{C}_{12}^{35}\text{Cl}_6\text{H}_4$ .

<sup>f</sup> No coexisting fragment ion.

highest relative abundances of labeled and unlabeled target compounds are selected as the parent ions, ions with the same  $m/z$  as the selected parent ions can be found (Table 2). For PCB 153 (a hexachlorinated biphenyl), because the only coexisting ion is  $m/z$  370 and the selected parent ions are  $m/z$  360 and 372 for unlabeled and labeled PCB 153, respectively, it is impossible to produce the same daughter ions for unlabeled and labeled PCB 153; as a result, there is no cross interference. On the other hand, none of the parent ions of the unlabeled PCB congeners are identical to the quantitation ions of labeled PCB counterparts (Table 2); therefore, no interference shall occur with quantitation of unlabeled PCBs due to the presence of  $^{13}\text{C}$ -labeled PCB counterparts. However, for  $^{13}\text{C}$ -labeled hepta- to deca-chlorinated PCB congeners, coexisting ions from their unlabeled PCB counterparts are present.

Therefore, the following discussions will focus on the interferences with quantitation of  $^{13}\text{C}$ -labeled PCBs from their unlabeled counterparts.

Because daughter ions are produced via dissociation of the parent ions of labeled PCB congeners often by losing two chlorine atoms [26–29], the probabilities for such a dissociation route for  $^{35}\text{Cl} + ^{35}\text{Cl}$  atom,  $^{35}\text{Cl} + ^{37}\text{Cl}$  and  $^{37}\text{Cl} + ^{37}\text{Cl}$  can be calculated with Eq. (5) (Table 3). It is apparent that the probability for loss of  $^{35}\text{Cl}$  from a selected ion of a labeled PCB congener is higher than that for loss of  $^{37}\text{Cl}$ . As a result, the  $P_2$  values with loss of two  $^{35}\text{Cl}$  atoms are the highest among all combinations. Similarly, the coexisting ion from an unlabeled PCB congener can also be dissociated by loss of two Cl atoms, and the probability ( $P_1$ ) can be computed accordingly. Due to the enrichment of  $^{37}\text{Cl}$  in these coex-

**Table 3**  
The selected parent ions of  $^{13}\text{C}$ -labeled PCB congeners, coexisting ions from their unlabeled counterparts, and their probability of losing chlorine atoms in the MS/MS mode.

Compound	Parent ion	Coexisting ion	Weight ( $m/z$ )	$P_1^a$			$P_2^b$		
				$^{35}\text{Cl}^{35}\text{Cl}^c$	$^{35}\text{Cl}^{37}\text{Cl}$	$^{37}\text{Cl}^{37}\text{Cl}$	$^{35}\text{Cl}^{35}\text{Cl}$	$^{35}\text{Cl}^{37}\text{Cl}$	$^{37}\text{Cl}^{37}\text{Cl}$
PCB 153	$^{13}\text{C}_{12}^{35}\text{Cl}_5^{37}\text{ClH}_4$	No <sup>d</sup>	372	0	0	0	0.67	0.33	0
PCB 180	$^{13}\text{C}_{12}^{35}\text{Cl}_6^{37}\text{ClH}_3$	$^{12}\text{C}_{12}^{37}\text{Cl}_7\text{H}_3$	406	0	0	1	0.71	0.29	0
PCB 202	$^{13}\text{C}_{12}^{35}\text{Cl}_6^{37}\text{Cl}_2\text{H}_2$	$^{12}\text{C}_{12}^{37}\text{Cl}_8\text{H}_2$	442	0	0	1	0.54	0.43	0.036
PCB 206	$^{13}\text{C}_{12}^{35}\text{Cl}_7^{37}\text{Cl}_2\text{H}$	$^{12}\text{C}_{12}^{35}\text{Cl}^{37}\text{Cl}_8\text{H}$	476	0	0.22	0.78	0.58	0.39	0.028
PCB 209	$^{13}\text{C}_{12}^{35}\text{Cl}_8^{37}\text{Cl}_2$	$^{12}\text{C}_{12}^{35}\text{Cl}_2^{37}\text{Cl}_8$	510	0.022	0.36	0.62	0.62	0.36	0.022

<sup>a</sup> The probability of the losing of two chlorine atoms from the selected coexisting ion of unlabeled PCB congener.

<sup>b</sup> The probability of the losing of two chlorine atoms from the selected parent ion of  $^{13}\text{C}$ -labeled congener.

<sup>c</sup>  $^{35}\text{Cl}^{35}\text{Cl}$  represents two  $^{35}\text{Cl}$  atoms,  $^{35}\text{Cl}^{37}\text{Cl}$  represents one  $^{35}\text{Cl}$  atom and one  $^{37}\text{Cl}$  atom, and  $^{37}\text{Cl}^{37}\text{Cl}$  represents two  $^{37}\text{Cl}$  atoms.

<sup>d</sup> No coexisting ion from its unlabeled PCB counterpart.

isting molecules, the  $P_1$  values for loss of two  $^{37}\text{Cl}$  atoms are higher than those for loss of two  $^{35}\text{Cl}$  atoms (Table 3). Because there is no coexisting ion for the parent ion of  $^{13}\text{C}$ -labeled PCB 153, no interference exists (as discussed above). Furthermore, there is also no interference with quantitation of  $^{13}\text{C}$ -labeled PCB 180 because its parent ion comprises six  $^{35}\text{Cl}$  atoms and one  $^{37}\text{Cl}$  atom. As a result,  $P_2$  of losing two  $^{37}\text{Cl}$  atoms was calculated as 0 (Table 3). However, the coexisting ion from unlabeled PCB 180 consists of seven  $^{37}\text{Cl}$  atoms, and it can produce daughter ions only with the loss of two  $^{37}\text{Cl}$  atoms. As a result,  $^{13}\text{C}$ -labeled and unlabeled PCB 180 cannot be dissociated to produce the same daughter ions (Table 4).

As far as  $^{13}\text{C}$ -labeled PCB 202 is concerned, it can be dissociated into three daughter ions ( $m/z$  372 with loss of two  $^{35}\text{Cl}$  atoms,  $m/z$  370 with loss of one  $^{35}\text{Cl}$  and one  $^{37}\text{Cl}$  atom and  $m/z$  368 with loss of two  $^{37}\text{Cl}$  atoms) with  $P_2$  values of 0.54, 0.43 and 0.036, respectively. In addition,  $P_1$  values of losing two  $^{35}\text{Cl}$  atoms ( $m/z$  364), one  $^{35}\text{Cl}$  and one  $^{37}\text{Cl}$  atom ( $m/z$  366) and two  $^{37}\text{Cl}$  atoms ( $m/z$  368) for unlabeled PCB 202 are 0, 0 and 1, respectively. When daughter ion  $m/z$  372 or 372 + 370 is selected as the quantitation ion, there is no interference from unlabeled PCB 202 with quantitation of  $^{13}\text{C}$ -labeled PCB 202. By contrast, when  $m/z$  368 + 370 + 372 was selected as the quantitation ion group, quantitation error occurred (Table 4). For  $^{13}\text{C}$ -labeled PCB 209, when the most abundant daughter ion ( $m/z$  440) was selected as the quantitation ion, there was

quantitation error due to the presence of coexisting daughter ions from unlabeled PCB 209 (Table 4). Herein, there were quantitation errors with different quantitation ions at five  $C_t$  values (from 25 to 500; Table 4).

Apparently, the quantitation errors for  $^{13}\text{C}$ -labeled PCB 153, 180 and 202 were all less than 15% with the use of any selected quantitation ions at five different  $C_t$  values. For  $^{13}\text{C}$ -labeled PCB 202, the quantitation error could reach 15% when the combination of three daughter ions was selected as the quantitation ion group at  $C_t = 500$ . For  $^{13}\text{C}$ -labeled PCB 209, when daughter ions  $m/z$  438 and 440 at  $C_t = 500$  and  $m/z$  436, 438 and 440 at  $C_t = 200$  and 500, the quantitation errors were all higher than 15% (Table 4). On the other hand,  $C_t$  values could be computed to satisfy the no-interference conditions for quantitation of five  $^{13}\text{C}$ -labeled mode compounds by Eq. (9). As a result, there is no constraint on the  $C_t$  levels for quantitation of  $^{13}\text{C}$ -labeled PCB 153 and 180 as long as the most abundant daughter ion or both daughter ions are chosen for quantitation (Table 4). Similarly, no interference was found with quantitation of  $^{13}\text{C}$ -labeled PCB 202 with quantitation ions of  $m/z$  372 and 370 + 372 and  $^{13}\text{C}$ -labeled PCB 206 with quantitation ion of 406  $m/z$  at any  $C_t$  levels. However, if daughter ions of 368 + 370 + 372  $m/z$  are employed as the quantitation ion group for  $^{13}\text{C}$ -labeled 202, 404 + 406 and 402 + 404 + 406  $m/z$  for  $^{13}\text{C}$ -labeled PCB 206, and 440, 438 + 440 and 436 + 438 + 440  $m/z$  for  $^{13}\text{C}$ -labeled PCB 209, respectively, the  $C_t$  values must be set at less than 3570, 2230, 500, 3410,

**Table 4**  
The theoretically predicted quantitation error ( $E$ (%)) when two chlorine atoms were lost from their parent ions with different quantitation ions and  $C_1/C_2$  ( $C_t$ ) levels for  $^{13}\text{C}$ -labeled PCB congeners in the MS/MS mode.

Compound	Quantitation ions	Coexisting ions	$E$ (%)					No interference <sup>b</sup>
			25 <sup>a</sup>	50	100	200	500	
PCB 153	302	No <sup>c</sup>	No	No	No	N	No	No constraint
	300 + 302	No	No	No	No	No	No	No constraint
PCB 180	336	No	No	No	No	No	No	No constraint
	334 + 336	No	No	No	No	No	No	No constraint
PCB 202	372	No	No	No	No	No	No	No constraint
	370 + 372	No	No	No	No	No	No	No constraint
	368 + 370 + 372	368	0.10	0.21	0.42	0.84	2.10	3570
PCB 206	406	No	No	No	No	No	No	No constraint
	404 + 406	404	0.17	0.34	0.67	1.35	3.36	2230
	402 + 404 + 406	402 + 404	0.74	1.5	3.0	5.9	15	500
PCB 209	440	440	0.11	0.22	0.43	0.86	2.2	3410
	438 + 440	438 + 440	1.2	2.4	4.7	9.5	24	312
	436 + 438 + 440	436 + 438 + 440	3.0	6.1	12	24	61	123

<sup>a</sup> Level of  $C_1/C_2$  ( $C_t$ ).

<sup>b</sup> Acceptable maximum  $C_t$  value to satisfy the no-interference condition when  $E$ (%) is set at 15%.

<sup>c</sup> There is no coexisting fragment ion and no interference.



**Table 5**

The square of the linear correlation coefficient ( $R^2$ ) and their relative standard deviation (RSD (%)) for five  $^{13}\text{C}$ -labeled PCB congeners in series A and B acquired in the MS/MS and SIS modes.

Compound	Series A <sup>a</sup>		Series B <sup>b</sup>	
	SIS mode	MS/MS mode	SIS mode	MS/MS mode
$^{13}\text{C}$ -PCB 153	0.998 ± 2.93 <sup>c</sup>	0.996 ± 7.19	0.999 ± 1.73	0.998 ± 3.56
$^{13}\text{C}$ -PCB 180	0.994 ± 10.2	0.990 ± 5.75	0.999 ± 4.45	0.998 ± 5.28
$^{13}\text{C}$ -PCB 202	0.997 ± 9.32	0.997 ± 4.45	0.990 ± 16.7	1.00 ± 1.42
$^{13}\text{C}$ -PCB 206	0.992 ± 12.6	0.998 ± 3.41	0.869 ± 28.7	1.00 ± 1.09
$^{13}\text{C}$ -PCB 209	0.995 ± 11.0	0.994 ± 6.44	0.756 ± 29.9	0.990 ± 6.00

<sup>a</sup> Series A is a series of solutions containing five levels (10, 20, 30, 40 and 50 ng/mL) of  $^{13}\text{C}$ -labeled PCB congeners and 40 ng/mL of their unlabeled counterparts as internal standards.

<sup>b</sup> Series B is a series of solutions containing five levels (10, 20, 30, 40 and 50 ng/mL) of  $^{13}\text{C}$ -labeled PCB congeners and 1000 ng/mL of their unlabeled counterparts as internal standards.

<sup>c</sup> Square of linear correlation coefficient ( $R^2$ ) ± relative standard deviation (RSD).

312 and 123 to satisfy the no-interference condition ( $E'(\%) < 15\%$ ) (Table 4).

#### 4.2. Experimental validation of the MS/MS approach with analyses of series A and B

Standard calibration curves of  $^{13}\text{C}$ -PCB 153, 180, 202, 206 and 209 in series A and B were established with their unlabeled counterparts as the internal standards obtained in both the SIS and MS/MS modes. A good linear relationship is assumed if a linear correlation coefficient ( $R^2$ ) > 0.99 and relative standard deviation (RSD) < 10% can be obtained. In the MS/MS mode, this criterion was satisfied for all the target compounds in both sets of standard solutions; good linear relationships were also achieved for series A in the SIS mode. Additionally, good linear relationships were obtained for  $^{13}\text{C}$ -PCB 153, 180 and 202 in series B in the SIS mode, but not for  $^{13}\text{C}$ -PCB 206 and 209 with the  $R^2$  values being 0.869 and 0.756 with RSD of 28.7% and 29.9%, respectively (Table 5). In the SIS mode, the quantitation errors were derived from partially overlapping mass profiles with their unlabeled PCB congeners [9]. Yang et al. [9] determined the theoretically maximum ratios of the unlabeled and  $^{13}\text{C}$ -labeled PCB congener concentrations ( $C_t$ ) for satisfying the condition of negligible quantitation interference with different quantitation ions for labeled PCB congeners with an acceptable quantitation error (e.g., 5%). Briefly, when  $C_t$  is less than 201.3 for the quantitation of  $^{13}\text{C}$ -labeled PCB 153 with quantitation ions of  $m/z$  370 + 372 + 374, 784.0 for  $^{13}\text{C}$ -labeled PCB 180 with quantitation ions ( $m/z$ ) of 406 + 408 + 410, 123.6 for  $^{13}\text{C}$ -labeled PCB 202 with quantitation ions ( $m/z$ ) of 440 + 442 + 444, 33.9 for  $^{13}\text{C}$ -labeled PCB 206 with quantitation ions ( $m/z$ ) of 474 + 476 + 478 and 12.3 for

$^{13}\text{C}$ -labeled PCB 209 with quantitation ions ( $m/z$ ) of 508 + 510 + 512, the relative quantitation error would be less than 5%. In the present study, the  $C_t$  value was set at 4, 2, 4/3, 1, and 4/5 for all target analytes in series A, which are substantially less than the values proposed by Yang et al. [9]. Therefore, interferences from partially overlapping mass profiles were negligible. Conversely, the  $C_t$  values from 20 to 100 in series B are less than the proposed values for  $^{13}\text{C}$ -labeled PCB 153, 180 and 202, but in some cases are higher than the proposed values for  $^{13}\text{C}$ -labeled PCB 206 (33.9) and 209 (12.3). As a result, poor linear relationship was found for  $^{13}\text{C}$ -labeled PCB 206 and 209.

On the other hand,  $R^2$  with > 0.99 and RSD with < 10% were observed for all target analytes in both series A and B in the MS/MS mode. Therefore, good linear correlations for all  $^{13}\text{C}$ -labeled PCB congeners of both series A and B were observed in the MS/MS mode (Table 5). This indicates that tandem mass spectrometry is a suitable tool to eliminate interferences derived from coeluting compound(s) with overlapping mass profiles (partially or completely).

#### 4.3. Experimental validation from analyses of spiked solutions

Series D with different values of  $C_t$  were analyzed with the MS/MS procedure in seven repeated runs. The concentrations of the five selected  $^{13}\text{C}$ -labeled PCB congeners ranged from 18.1 ± 1.2 to 30.4 ± 1.4 ng/mL in all spiked solutions with an initial spiking concentration of 20 ng/mL when the most and second most abundant daughter ions were selected as the quantitation ions (Table 6). The  $E'(\%)$  values were within the range of 4.4 ± 2.9% to 15.5 ± 6.3% except for  $^{13}\text{C}$ -PCB 209 at  $C_t = 500$  (Table 6).  $E'(\%)$  value of  $^{13}\text{C}$ -

**Table 6**

Measured recoveries (%) and quantitation error of  $^{13}\text{C}$ -labeled PCB congeners from a group of spiked solutions with different levels of their unlabeled PCB counterparts by seven repeated runs in the MS/MS mode.

Compound	0 <sup>a</sup>	25 <sup>a</sup>	50 <sup>a</sup>	100 <sup>a</sup>	200 <sup>a</sup>	500 <sup>a</sup>
Measured concentration (ng/mL)						
PCB 153	18.1 ± 1.2 <sup>b</sup>	19.3 ± 2.4	18.8 ± 2.9	20.2 ± 2.7	19.1 ± 2.6	19.1 ± 2.2
PCB 180	20.2 ± 1.6	18.8 ± 2.5	19.9 ± 2.9	19.0 ± 2.9	19.5 ± 2.3	19.8 ± 3.5
PCB 202	22.5 ± 2.5	22.0 ± 2.7	20.2 ± 2.7	22.8 ± 1.7	23.9 ± 2.3	22.6 ± 2.5
PCB 206	22.6 ± 2.6	23.5 ± 3.3	23.3 ± 2.4	23.6 ± 2.2	20.6 ± 1.4	23.1 ± 3.4
PCB 209	21.7 ± 1.6	20.4 ± 3.2	23.6 ± 2.1	23.6 ± 3.3	23.6 ± 2.3	30.4 ± 1.4
Measured quantitation error						
PCB 153	5.2 ± 3.8 <sup>c</sup>	9.4 ± 7.2	12.5 ± 7.2	11.2 ± 5.8	12.3 ± 3.8	9.1 ± 5.6
PCB 180	6.9 ± 2.9	11.8 ± 4.5	11.9 ± 6.5	11.8 ± 8.0	9.6 ± 6.0	15.5 ± 6.3
PCB 202	8.1 ± 7.0	10.1 ± 5.6	11.2 ± 6.0	4.7 ± 5.3	8.4 ± 3.6	9.0 ± 5.5
PCB 206	9.8 ± 4.7	10.5 ± 8.1	9.1 ± 3.0	7.4 ± 4.4	5.6 ± 2.6	12.0 ± 7.4
PCB 209	5.9 ± 3.9	13.0 ± 7.4	6.8 ± 4.7	11.8 ± 6.2	7.3 ± 5.6	52.2 ± 6.9

<sup>a</sup> The values of  $C_t = 0$ , and 25, 50, 100, 200 and 500 represent the concentrations of  $^{13}\text{C}$ -labeled PCB congeners spiked at 20 ng/mL and the concentrations of unlabeled PCB counterparts at 0, 500, 1000, 2000, 4000 and 10,000 ng/mL.

<sup>b</sup> Represents the measured recovery ± standard relative derivation.

<sup>c</sup> Represents the measured quantitation error ± standard relative derivation.

labeled PCB 209 was estimated at 24% at  $C_t = 500$  with quantitation ions of  $m/z$  438 + 440, which is less than half of  $E'$  (%) value ( $52 \pm 7\%$ ). This can be attributed to a combination of instrumental analytical uncertainty and interference from coexisting ions. Instrumental analytical uncertainty might be significant in the MS/MS approach, because  $E'$  (%) values for the spiked solutions without unlabeled PCB 209 ranged from 0.5% to 11.6% with an average value of 5.9% (Table 6). More importantly,  $E'$  (%) with  $^{13}\text{C}$ -labeled PCB 180 at  $C_t = 500$  was 16%, which could be attributed to instrumental analytical uncertainty. In comparison with the SIS mode [9], MS/MS techniques appear to be able to minimize quantitation interference for the selected  $^{13}\text{C}$ -labeled PCB with partially overlapping ion profiles with their unlabeled PCB counterparts. Therefore, use of the analytical scheme to quantify coeluting PCB counterparts with partially overlapping ion profile would gain optimal results.

## 5. Conclusions

The present study utilized probability and combination theory to explore the possibility of using the MS/MS mode inherited in tandem mass spectrometry to minimize quantitation interferences resulting from coexisting ion fragments. An algorithm was developed to predict quantitation errors, and five unlabeled and  $^{13}\text{C}$ -labeled PCB congener counterparts were used as model compounds to validate the theoretical predictions. Good agreements between experimentally measured errors and theoretical predictions were found for quantitation of  $^{13}\text{C}$ -labeled PCB congeners, indicating that MS/MS is superior to conventional MS in minimizing quantitation interferences resulting from this specific situation. It should be noted that Eq. (9) can be applicable to any other similar systems in combination with the two-component model [9,15,16].

## Acknowledgements

Financial support of the present study was provided by China Postdoctoral Science Foundation funded project (20080440709)

and the National Natural Science Foundation of China (40903039 and 40821003). This is contribution No. IS-1163 from GIGACS.

## References

- [1] S.D. Cooper, M.A. Moseley, E.D. Pellizzari, *Anal. Chem.* 57 (1985) 2469.
- [2] E.H. Lee, G.D. Oliver, *Anal. Chem.* 31 (1959) 1925.
- [3] P. Dewsbury, S.F. Thornton, D.N. Lerner, *Environ. Sci. Technol.* 37 (2003) 1392.
- [4] C.C. Sweeley, W.H. Elliott, I. Fries, R. Ryhage, *Anal. Chem.* 38 (1966) 1549.
- [5] J.F. Pickup, K. McPherson, *Anal. Chem.* 48 (1976) 1885.
- [6] P. Schieberle, W. Grosch, *J. Agric. Food Chem.* 35 (1987) 252.
- [7] L.K. Ackerman, G.R. Wilson, S.L. Simonich, *Anal. Chem.* 77 (2005) 1979.
- [8] J. Malavia, F.J. Santos, M.T. Galceran, *J. Chromatogr. A* 1056 (2004) 171.
- [9] Z.Y. Yang, E.Y. Zeng, J.Z. Wang, B.X. Mai, *J. Chromatogr. A* 1116 (2006) 265.
- [10] S.S. Verenitch, A.M.H. deBruyn, M.G. Ikonomou, A. Mazumder, *J. Chromatogr. A* 1142 (2007) 199.
- [11] M.J. Charles, Y. Tondeur, *Environ. Sci. Technol.* 24 (1990) 1856.
- [12] J.-F. Focant, E.J. Reiner, K. MacPherson, T. Kolic, A. Sjödin, D.G. Patterson, S.L. Reese, F.L. Dorman, J. Cochran, *Talanta* 63 (2004) 1231.
- [13] S.A. Mjøs, *Anal. Chim. Acta* 488 (2003) 231.
- [14] C. Naert, S.D. Saeger, C.V. Peteghem, *Rapid Commun. Mass Spectrom.* 18 (2004) 2317.
- [15] E.Y. Zeng, C.C. Chou, C. Yu, *Anal. Chem.* 74 (2002) 4513.
- [16] E.Y. Zeng, C.C. Yu, *Environ. Sci. Technol.* 30 (1996) 322.
- [17] T.R. Schwartz, D.E. Tillitt, K.P. Feltz, P.H. Peterman, *Chemosphere* 26 (1993) 1443.
- [18] M. Lausevic, J.B. Plomley, X. Jiang, R.E. March, *Eur. J. Mass Spectrom.* 1 (1995) 149.
- [19] E.d.H.N. Viseux, B. Domon, *Anal. Chem.* 69 (1997) 3193.
- [20] Z.Y. Yang, E.Y. Zeng, H. Xia, J.Z. Wang, B.X. Mai, K.A. Maruya, *J. Chromatogr. A* 1116 (2006) 240.
- [21] H.T. Tang, *Spectroscopic Identification of Organic Compounds*, Peiking University Publication, Beijing, 1994.
- [22] R. Serrano, M. Barreda, M.A. Blanes, *Mar. Pollut. Bull.* 56 (2008) 963.
- [23] A. Derouiche, M.R. Driss, J.-P. Morizur, M.-H. Taphanel, *J. Chromatogr. A* 1138 (2007) 231.
- [24] R.F. Lopshire, J.T. Watson, C.G. Enke, *Toxicol. Ind. Health* 12 (1996) 375.
- [25] L. Zupančič-Kralj, J. Marsel, B. Kralj, D. Žigon, *Analyst* 119 (1994) 1129.
- [26] M. Mandalakis, M. Tsapakis, E.G. Stephanou, *J. Chromatogr. A* 925 (2001) 183.
- [27] J.B. Plomley, M. Lausevic, R.E. March, *Mass Spectrom. Rev.* 19 (2000) 305.
- [28] M. Lausevic, M. Splendore, R.E. March, *J. Mass Spectrom.* 31 (1996) 1244.
- [29] F.J. Santos, M.T. Galceran, J. Caixach, X. Huguët, J. Rivera, *Rapid Commun. Mass Spectrom.* 10 (1996) 1774.